

Effect of Fluoride Ion on the Corrosion of 304 Stainless Steel in $(\text{NH}_4)_2\text{SO}_4$ Solution Containing Chloride Ions

Zhengwei Luo, Yin Zhang, Yongzhang Zhou, Zhouyang Lian^{*}, Wuji Wei^{*}

School of Environmental Science and Engineering, Nanjing Tech University, 30[#] Puzhu South Road, Nanjing 211816, P. R. China

^{*}E-mail: wjwei@njtech.edu.cn (W. Wei), lianzy1985@163.com (Z. Lian)

Received: 8 January 2021 / Accepted: 7 March 2021 / Published: 31 March 2021

The corrosion behavior of stainless steel in contact with an ammonia desulphurization slurry, which contains a high concentration of both fluoride ions (F^-) and chloride ions (Cl^-), affects the commercialization of the ammonia desulphurization technology. In this paper, 304 stainless steel was taken as a typical stainless steel sample to explore the influence of F^- on its corrosion behavior in a simulated ammonia desulfurization slurry. The open circuit potential, polarization voltage, polarization current, cyclic voltammograms, electrochemical impedance spectroscopy, and Mott-Schottky plots, for different F^- concentrations, have been studied using electrochemical methods. At the same time, the influence of different F^- concentrations on the corrosion of stainless steel was studied by an immersion test, and the specimens were characterized by scanning electron microscopy and X-ray photoelectron spectroscopy. The experimental results show that in the simulated ammonium desulfurization slurry, at a given concentration of Cl^- , low concentrations of F^- aggravated the corrosion of stainless steel, while a high concentration of F^- (the molar ratio of F^- to Cl^- is higher than 10) produced significant corrosion inhibition. The reason may be that F^- can combine with H^+ , preventing the pH of the solution from becoming too low, and simultaneously, F^- can also react with metal ions to form insoluble sediments, which prevent the aggravation of the corrosion process.

Keywords: Ammonia desulfurization; stainless steel; fluoride; corrosion; inhibition

1. INTRODUCTION

Flue gas ammonia desulphurization slurry contains both chloride ion (Cl^-) and fluoride ion (F^-) from coal burning, and is a typical example of a Cl^- and F^- mixed system [1]. While various systems contain both Cl^- and F^- , such as proton exchange membrane fuel cells [2], conversion fluid [3], oral saliva [4], and phosphoric acid processing fluid [5], the ammonia desulfurization slurry is more complex, contains a higher concentration of Cl^- and F^- , and is larger in volume. The impact of Cl^- has

been more widely studied as it shows high chemical activity and is an important factor affecting metal corrosion, especially stainless steel corrosion [6]. Relatively speaking, the influence of F^- on stainless steel corrosion has been less studied [7]. In general, F^- causes uniform corrosion on the entire metal surface while Cl^- mainly causes local corrosion [8-10]. The study of corrosion of stainless steel, by these two ions, in the ammonia desulphurization equipment, can help identify appropriate anti-corrosion strategies for stable operation and commercialization of the technology.

According to the state of the art, the effect of F^- on the corrosion of stainless steel remains inconclusive. On the one hand, studies indicate that F^- might lead to intensified general corrosion or localized corrosion of stainless steel [11]. Martinović *et al.* [12] found that under acidic conditions, 0.1 mol/L of F^- could promote the dissolution of a passivation film on the surface of 304 stainless steel. Yang *et al.* [2] studied the influence of F^- on the corrosion of 316 stainless steel in fuel cell electrolytes, and the results showed that a high concentration of F^- aggravated the pitting of stainless steel. On the other hand, F^- is also known to have an inhibitory effect on the corrosion of stainless steel [13]. Pardo *et al.* [14] proposed that a complexation reaction of F^- with Fe^{3+} occurs, resulting in the formation and deposition of a layer of Na_3FeF_6 on the metal surface, which prevents acidification caused by hydrolysis of metal ions; thus, protecting the steel surface. Mirjalili *et al.* [4] showed that the addition of F^- in simulated saliva alleviated the pitting corrosion of 304 stainless steel and increased the corrosion potential of 304 stainless steel; however, the specific mechanism was not investigated. Therefore, it can be concluded that F^- has different effects on the corrosion process of stainless steel in different systems and under different ionic concentration conditions.

In the presence of Cl^- and F^- , the simultaneous impact of both ions, on the corrosion of stainless steel, is more complex than that of each ion alone [9, 15]. According to Wang *et al.* [16], both Cl^- and F^- tend to result in an aggravated yet uniform corrosion of 316 stainless steel, where F^- plays a weaker role in promoting local corrosion. In some cases, F^- may prevent the damage of the passivation film of the stainless steel surface which is being attacked by Cl^- ; thus, inhibiting the corrosion of stainless steel [17]. Yang *et al.* [18] showed that while F^- might exist as HF , HF_2^- , $H_2F_3^-$, and $H_3F_4^-$ in an acidic aqueous solution which results in uniform corrosion of stainless steel, F^- could instead promote the formation of a passivation film on the surface of stainless steel and reduce the corrosion rate under certain conditions. Martinović *et al.* [12] found that at a certain pH and F^- concentration, the applied anodic polarization current could result in the formation of an oxide film on the surface of 304 stainless steel. Molchan *et al.* [19] treated 304 stainless steel with fluorine-containing ionic liquids and found that passivation films, composed of FeO , Fe_2O_3 , Cr_2O_3 , $Cr(OH)_3$, and small amounts of NiO and $Ni(OH)_2$, formed on the surface of stainless steel. Therefore, in literature, the corrosion effect of the two coexisting halide ions on stainless steel has been attributed to ion concentration, the ratio between two ions, and the composition of the material in contact with the mixed halides [17]; however, the specific mechanism for this phenomenon has not been fully identified yet.

Since a high concentration of Cl^- and F^- tend to accumulate in flue gas ammonia desulphurization slurry, it is imperative to examine the impact of concentration of F^- and the ratio of the concentrations of F^- and Cl^- , on the corrosion of stainless steel. By having a clear understanding of the corrosion mechanism of the ammonia desulphurization equipment, safe and stable operation of the equipment can be achieved and higher desulfurization efficiency of the flue gas can be guaranteed. In

this work, by adjusting the concentration of F^- and the ratio of concentration of F^- and Cl^- , the corrosion behavior of austenitic 304 stainless steel, in different solution systems, has been studied by electrochemical analysis and immersion tests. Furthermore, based on the results obtained from the material characterization, a corrosion mechanism has been proposed.

2. EXPERIMENTAL SECTION

2.1. Materials

A test solution simulating the conditions of the desulfurization slurry was prepared with NH_4F , NH_4Cl , and $(NH_4)_2SO_4$, with analytical purity, as purchased from Sinopharm Chemical Reagent Co., Ltd. To evaluate the influence of F^- on the corrosion of 304 stainless steel, the simulated ammonia desulfurization slurry was used in the immersion test with 30% (w/v) of $(NH_4)_2SO_4$, 0.1 M of Cl^- , and the concentration of F^- was varied from 0 to 1 M. As the metal specimen undergoing corrosion, 304 austenitic stainless steel was used, and its components are shown in Table 1. The electrode used in the electrochemical experiments was cylindrical, with a cross-sectional area of 1.0 cm^2 ; it consisted of a wire welded at one end of the electrode, which was then sealed with epoxy and exposed at the other end. Before the experiment, the electrodes were polished to 800 mesh, step by step, with sandpaper, sequentially cleaned with anhydrous ethanol and acetone, and dried.

Table 1. The nominal chemical composition of the tested 304 stainless steel (wt%).

Cr	Ni	C	S	Si	Mn	P	Fe
18.23	8.10	0.04	0.002	0.35	1.10	0.036	balance

2.2. Electrochemical tests

Electrochemical measurements were carried out on a CHI 660C electrochemical workstation (Shanghai Chenhua Instrument Co., Ltd.). The experiment adopted a three-electrode system, with a saturated calomel electrode as the reference electrode and a platinum electrode as the auxiliary electrode. The potential values in this paper are all relative to the saturated calomel electrodes unless otherwise stated. Before the electrochemical measurements were carried out, the electrode was immersed in the test solution, which was at $50\text{ }^\circ\text{C}$, for 30 min. The potentiodynamic measurements were conducted at a scanning rate of 1 mV/s , with a reverse sweep when the voltage reached 0.8 V . The cyclic voltammetry measurements were carried out at a scan rate of 50 mV/s . Electrochemical impedance spectra were obtained at open circuit potential (OCP) within a frequency range of $100\text{ kHz} \sim 0.01\text{ Hz}$. The amplitude of the sinusoidal perturbation signal was 5 mV . The test results were analyzed using the Zview software. The Mott-Schottky test was carried out after the electrode was polarized at 0.3 V for half an hour. The test was conducted at a frequency of 1 kHz , a sine wave

amplitude of 5 mV, within a potential range of -0.7 V ~ 0.8 V relative to the reference electrode, where the potential interval was 50 mV. The scanning was carried out from high potential to low potential.

2.3. Immersion test

A stainless steel specimen of dimensions $50 \times 25 \times 2 \text{ mm}^3$ was used. After polishing it step by step with SiC sandpaper to 800 mesh, the specimens were cleaned successively with deionized water, anhydrous ethanol, and acetone, blow-dried by cold air, and placed in a dryer. After 24 hours, the dried specimens were measured and weighed. The blank specimens were cleaned, weighed according to the same procedure and were taken as the control group. The metal corrosion rate was calculated by the change in the mass of the stainless steel specimens, according to the following equation:

$$V = \frac{8.76 \cdot (w_1 - w_2)}{\rho \cdot S \cdot t} \quad (1)$$

where V is the corrosion rate (mm/y), W_1 is the initial mass of the specimens (g), W_2 is the mass of specimens after corrosion (g), ρ is the metal density (g/cm^3), S is the surface area of specimens (m^2), and T is the testing time (h). Each measurement was obtained by averaging results for at least three samples.

The morphology and surface elements of the corrosion specimens were analyzed by scanning electron microscopy (SEM, S-3400N II, Hitachi) and X-ray photoelectron spectroscopy (XPS, PHI 5000 VersaProbe, ulvac-PHI). The X-ray source for XPS was Al (1486.6 eV), with a power of 150 W (15 kV, 10 mA). The binding energy of the elements was calibrated by C1s at 284.6 eV, and the energy spectra of each element were analyzed using the XPSPeak 4.1 software.

3. RESULTS AND DISCUSSION

3.1. Electrochemical study of the role of F^- and F^-/Cl^- ratio

In $(\text{NH}_4)_2\text{SO}_4$ (30%, w/v) solutions containing a fixed concentration of 0.1 M Cl^- , F^- concentrations, varying from 0 to 1.0 M, were added to investigate the effect of F^- on the corrosion behavior of 304 stainless steel. Figure 1 shows the trend of OCP of the 304 stainless steel specimens under different F^- concentrations. The OCP was seen to increase slowly and finally reached a relatively stable state, indicating that the passivated layer on the stainless steel surface and the equilibrium potential at the liquid-solid interface gradually stabilized to a quasi-steady state [20]. When F^- concentration increased along 0.01, 0.1, 0.5, and 1 M, the time needed to stabilize the OCP was shortened, and the final stable potential was less negative than that without the addition of F^- . This indicated that the passivation film on the stainless steel surface was more stable after adding F^- [21].

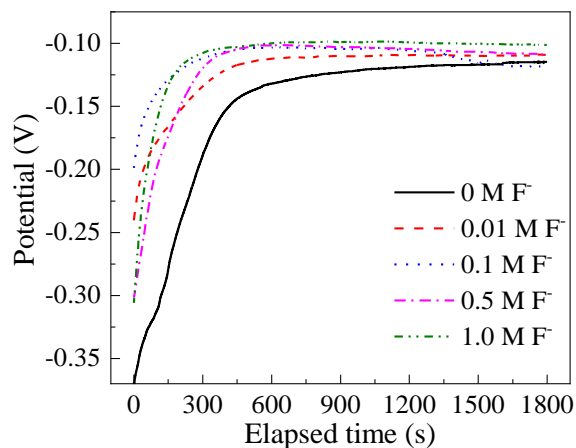


Figure 1. OCP variations for 304 stainless steel in bulk solutions (30% $(\text{NH}_4)_2\text{SO}_4$ (w/v), 0.1 M Cl^-) with F^- concentration from 0 M to 1.0 M.

The potentiodynamic polarization curves of 304 stainless steel under different F^- concentrations are shown in Figure 2(a). It can be seen that with the increase in F^- concentration, no obvious active dissolution peak appeared in the polarization curves. When the polarization potential increased to about 0.75 V, the polarization current for all the different F^- concentrations increased rapidly, which can be attributed to the oxidation of Cr(III) to Cr(VI) on the stainless steel surface [16]. The effects of different F^- concentrations on the polarization potential and polarization current of 304 stainless steel were summarized and compared in Figure 2(b). At F^- concentrations lower than 0.7 M, the polarization potential did not change too much with the increase of F^- concentration. When the F^- concentration was higher than 0.7 M, the polarization potential decreased significantly. The polarization current was seen to increase and then decrease with the F^- concentration; *i.e.*, at F^- concentration ranging from 0 M to 0.1 M, the corrosion current density increased slightly from 2.387×10^{-5} A to 3.202×10^{-5} A, and above 0.1 M of F^- , the corrosion current density gradually decreased. When the concentration of F^- reached 1.0 M, the corrosion current density had decreased significantly to 0.782×10^{-5} A and was much lower than that obtained without addition of F^- .

In terms of the molar ratio of F^- to Cl^- , when it was greater than 5, the corrosion of stainless steel showed an inhibitory effect and for a higher molar ratio, *i.e.*, 10, the inhibitory effect was significant. Therefore, the effect of F^- on the corrosion of 304 stainless steel was closely related to its concentration. At low concentrations, F^- tends to promote corrosion, and at high concentration, F^- inhibits corrosion of stainless steel [17].

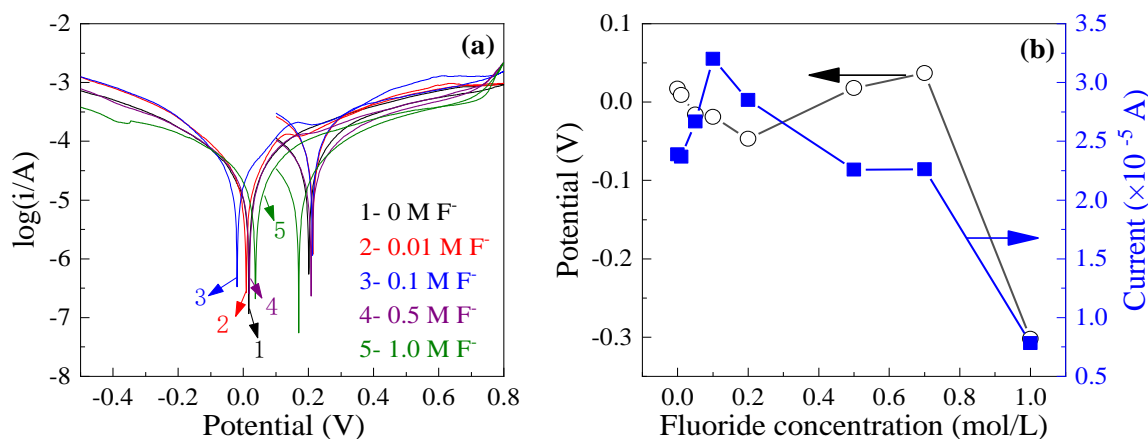


Figure 2. Potentiodynamic polarization curves of 304 stainless steel in bulk solution (30% (NH₄)₂SO₄ (w/v), 0.1 M Cl⁻) in presence of different concentration of F⁻ ions (a) and corrosion potential and corrosion current (b).

The cyclic voltammograms of 304 stainless steel, at different F⁻ concentrations, are shown in Figure 3. With the increase of F⁻ concentration, the area of the hysteresis loop was seen to decrease gradually, suggesting that the pitting tendency of the 304 stainless steel surface decreased. According to Wang *et al.* [16], F⁻ adsorption on the surface of stainless steel tends to hinder the adsorption of Cl⁻; thus, reducing the damage to the passivation film. Thus, the surface can be quickly repassivated even if defects occur in some areas.

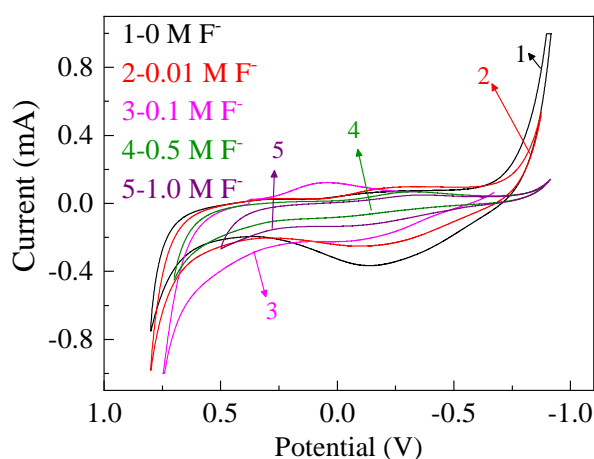


Figure 3. Cyclic voltammograms of 304 stainless steel in bulk solution (30% (NH₄)₂SO₄ + 0.1 M Cl⁻) in presence of different concentration of F⁻ ions.

Nyquist plots of electrochemical impedance spectra of 304 stainless steel at different F⁻ concentrations are fitted and shown in Figure 4. When F⁻ was added to the solution, the impedance was lower than that in the absence of F⁻; however, when F⁻ concentration was 1.0 M, the impedance increased. Kocijan *et al.* [11] showed that in artificial saliva with a NaF concentration of 1000 mg/L,

the impedance value of 316L stainless steel decreased compared with that without NaF. Wang *et al.* [16] studied the influence of F⁻ on the impedance of stainless steel at different Cl⁻ concentrations. The results showed that in the range of Cl⁻ concentration of 0 mM ~ 600 mM, the addition of F⁻, whether at 0.05 mM and 5 mM concentration, reduced the impedance of stainless steel. The fitted electrochemical impedance parameters (Table 2) show that with the increase in F⁻ concentration from 0 M to 0.5 M, the charge-transfer resistance (*R*_{ct}) decreased from 36471 Ω cm² to 17415 Ω cm². Furthermore, as the F⁻ concentration increased to 1.0 M, *R*_{ct} increased to 57706 Ω cm². This indicates that when F⁻ concentration is low, relative to Cl⁻, the corrosion of stainless steel tends to be accelerated. However, when the molar ratio of F⁻ to Cl⁻ is high, the impedance value rises, indicating that the corrosion resistance of stainless steel is accelerated, which is consistent with the potentiometric polarization results.

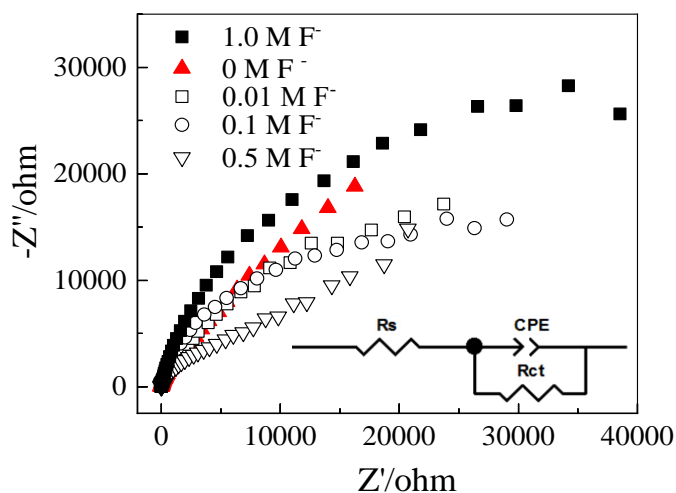


Figure 4. Nyquist plots of 304 stainless steel in bulk solution (30% NH₄)₂SO₄ + 0.1 M Cl⁻) with different F⁻ concentrations (inset shows the equivalent electrical circuit used for the fitting of impedance spectra).

Table 2. The fitted electrochemical impedance parameters of 304 stainless steel with different F⁻ concentrations (30% NH₄)₂SO₄ + 0.1 M Cl⁻).

F ⁻ concentration (M)	<i>R</i> _s (Ω cm ²)	CPE-T	CPE-P	<i>R</i> _{ct} (Ω cm ²)
0	0.53244	0.00024122	0.83346	36471
0.01	0.46214	0.00018297	0.83741	34502
0.1	0.39281	0.00010413	0.86780	33569
0.5	0.38574	0.00012436	0.84538	17415
1	0.42627	0.000083226	0.88548	57706

The Mott-Schottky test was carried out under different F^- concentrations, as shown in Figure 5. The semiconductor properties of stainless steel passivation films can be described by the Mott-Schottky theory [22, 23]. For n-type semiconductors:

$$\frac{1}{C^2} = \frac{2}{\varepsilon \varepsilon_0 e N_D} \left(E - E_{fb} - \frac{kT}{e} \right) \quad (2)$$

Additionally, for p-type semiconductors:

$$\frac{1}{C^2} = -\frac{2}{\varepsilon \varepsilon_0 e N_A} \left(E - E_{fb} - \frac{kT}{e} \right) \quad (3)$$

where, C is the space charge layer capacitance of the oxide film, ε is the relative dielectric constant of the oxide film, ε_0 is the vacuum dielectric constant, e is the electron charge, N_D and N_A are the electron donor and the electron acceptor concentrations, respectively, E is the external potential, E_{fb} is the flat potential, K is Boltzmann constant, and T is the thermodynamic temperature. The electronic properties of the metal surface passivation films were closely related to the capacitance of the space charge layer.

The Mott-Schottky plots in Figure 5 show that the amount of space charge of the passivation film tends to show significant variations with increase in potential; thus, the analysis is divided into three intervals according to the potential. Within the potential range of $-0.7 \text{ V} \sim -0.2 \text{ V}$, the slope of the curves was negative, indicating that the passivation film on the stainless steel surface is characterized as a p-type semiconductor [24]. As the concentration of F^- increased, the slope of the curve gradually decreased, indicating that the electron acceptor density gradually decreased. At this point, it was more difficult for Cl^- to adsorb and bind to the surface of the passivation film; thus, the pitting resistance of the stainless steel surface was enhanced.

Within the range of potential of $-0.2 \text{ V} \sim 0.4 \text{ V}$, the slope of the curves was positive; hence, the passivation film on the stainless steel surface behaves as an n-type semiconductor. When the concentration of F^- was below 0.1 M , the slope of the curve and the electron donor density did not change significantly. However, when the concentration of F^- increased to 0.5 and 1.0 M , the slope of the curve increased, indicating that the electron donor density also decreased. Within an applied potential range of $0.4 \text{ V} \sim 0.8 \text{ V}$, the slope of the curve was negative, *i.e.*, the passivation film on the stainless steel surface is characterized by a p-type semiconductor. The electron acceptor density was also lower when F^- concentration was 0.5 and 1.0 M . In general, a relatively high concentration of F^- can protect the passivation film on the surface of stainless steel and prevent it from being damaged by Cl^- .

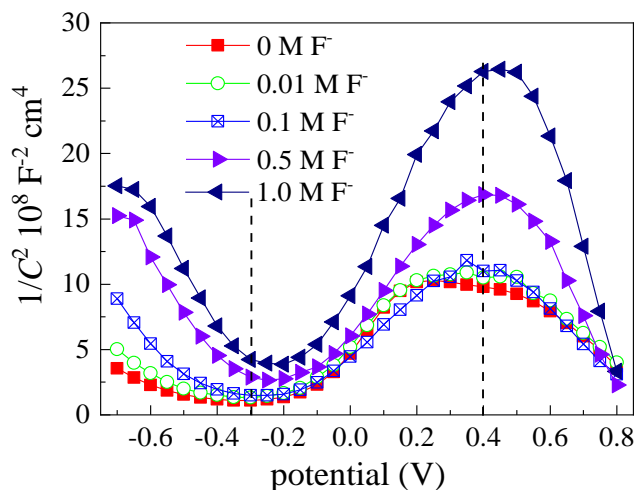


Figure 5. Mott-Schottky plots for 304 stainless steel with different concentrations of F^- (30% $(NH_4)_2SO_4 + 0.1 M Cl^-$).

3.2. Results obtained from immersion test

According to the above electrochemical experiments, F^- has a certain inhibitory effect on the corrosion caused by Cl^- , which may be related to the difference between the properties of F^- and Cl^- [7]. Therefore, the impact of the individual F^- and Cl^- concentrations, on the pH of the $(NH_4)_2SO_4$ solution, have been discussed.

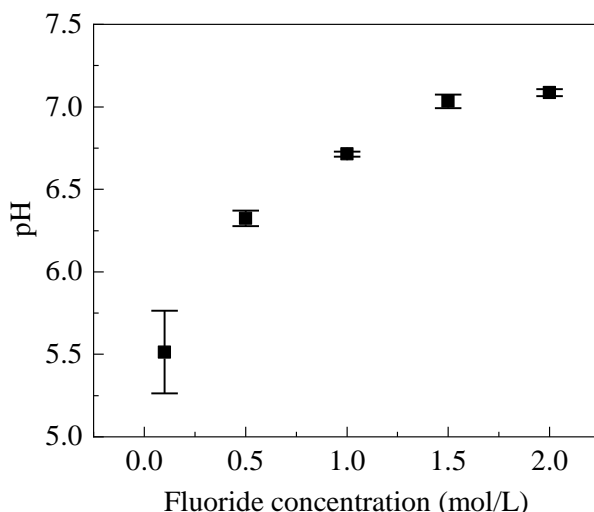


Figure 6. Influence of F^- concentration on the pH of the $(NH_4)_2SO_4$ (30%, w/v) solution.

Different concentrations of NH_4F were added to the solution with a 30% (w/v) $(NH_4)_2SO_4$ to investigate the effect of different concentrations of F^- on the pH of the solution. $(NH_4)_2SO_4$ belongs to the strong acid and weak base salt group and after hydrolysis in aqueous solution, the solution becomes

weakly acidic; thus, the solution was acidic in the absence of F^- (Figure 6). With the concentration of F^- increasing from 0.1 M to 2.0 M, the pH of the solution gradually increased to about 7.0. It has been reported that after NaF is added into the mixed solution of $MgSO_4$ and $Mg(NO_3)_2$, the pH of the solution showed similar changes [25]. Sekine *et al.* [26] have reported the effect of KF addition on the pH of a 0.01 M H_2SO_4 solution, and the results were similar to those obtained from this study.

Different solutions were prepared by adding different concentrations of Cl^- to $(NH_4)_2SO_4$ (30%, w/v) solutions with a fixed F^- concentration of 0.5 M; the corresponding evolution of pH of the solutions is shown in Figure 7. When the Cl^- concentration was below 0.5 M, the pH of the solution was relatively stable. The pH of the solution decreased slightly with the increase of Cl^- concentration and these results are consistent with the findings of Sekine *et al.* [26].

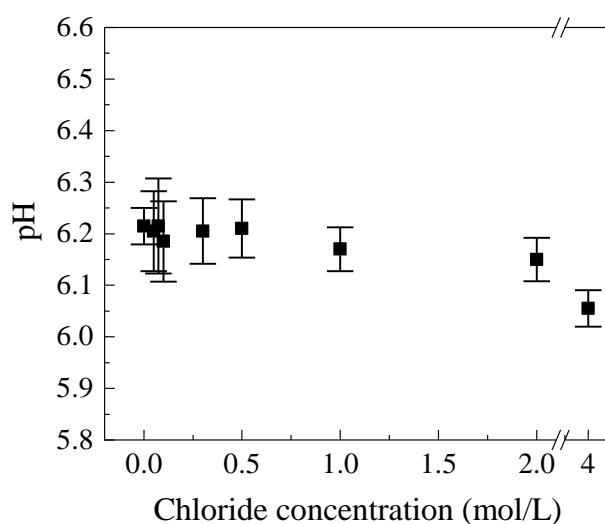


Figure 7. Influence of Cl^- concentration on the pH of a $(NH_4)_2SO_4$ (30%, w/v) solution containing 0.5 M F^- .

The effects of the two halide ions on the pH of solution can be attributed to their physicochemical properties. The dissociation of hydrohalic acid can be expressed as:



$$Ka = \frac{[H^+][X^-]}{[HX]} \quad (5)$$

$$pKa = pH - \lg \frac{[X^-]}{[HX]} \quad (6)$$

$$pH = pKa - \lg \frac{[X^-]}{[HX]} \quad (7)$$

where X represents the halide ion.

The dissociation constants of the four hydrohalic acids are shown in Table 3, which shows that the dissociation constant of F^- is significantly higher than that of other halide ions. For proton donors, the larger is the pKa , the smaller is the Ka , *i.e.*, the less free H^+ available in the solution, the higher is its pH. When the pH is lower, the corrosion rate of stainless steel tends to be higher. Therefore, a high concentration of F^- can cause the pH of the solution to be at a high value; thus, reducing the corrosion

of stainless steel. F^- does not have the ability, like that of oxyanions such as chromate and nitrate ions, which can form or strengthen passivation films on the surface of stainless steel; furthermore, the ability of F^- to regulate pH may be one of the reasons for its corrosion inhibition [17].

Table 3. Dissociation constants of different hydrogen halides.

	HF	HCl	HBr	HI
pK_a	3.2	-8.0	-9.0	-10.0

The influence of F^- on the corrosion rate of 304 stainless steel was investigated by adding different concentrations of NH_4F into the $(NH_4)_2SO_4$ (30%, w/v) solution. As shown in Figure 8, with the increase of F^- concentration, the corrosion rate of stainless steel does not change significantly and is always less than 0.0004 mm/y, indicating that F^- does not cause uniform corrosion of 304 stainless steel. In the $(NH_4)_2SO_4$ solution system, it is also possible that SO_4^{2-} has a strong corrosion inhibition effect on stainless steel [27, 28]. In conclusion, under these experimental conditions, the increase of F^- concentration to 1 M does not increase the corrosion rate of 304 stainless steel; hence, it does not promote the uniform corrosion of stainless steel.

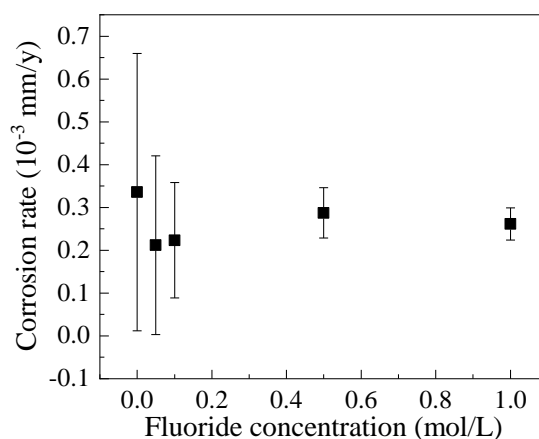


Figure 8. Influence of F^- concentration on the corrosion rate of 304 stainless steel in the immersion test ($(NH_4)_2SO_4$ (30%, w/v), 0.1 M Cl^-).

In addition, different concentrations of Cl^- were added to two different $(NH_4)_2SO_4$ (30%, w/v) solutions, *i.e.*, in absence and presence of 0.5 M F^- , and the corrosion rate of the stainless steel specimens is shown in Figure 9. Figure 9(a) shows the change of corrosion rate of stainless steel with Cl^- concentration in the absence of F^- . The corrosion rate of stainless steel increased from 0.009 mm/y to 0.059 mm/y with the concentration of Cl^- ranging from 0 M to 2 M. When the Cl^- concentration increased to 4 M, the corrosion rate reached 0.11 mm/y.

In the solution containing F^- concentration of 0.5 M (Figure 9(b)), the corrosion rate of stainless steel was lower than that without F^- and did not change significantly for a Cl^- concentration

range of 0 M ~ 2 M. When the Cl^- concentration was 4 M, the corrosion rate of stainless steel was 0.03 mm/y, which was far lower than that without F^- . However, for 4 M of Cl^- , there were obvious pitting holes on the surface of the specimen (inset in Figure 9(b)). This indicates that when the concentration of Cl^- was much higher than F^- , even though the uniform corrosion of stainless steel could be significantly inhibited, local corrosion still occurred. Thus, the inhibition effect of F^- is a function of its concentration and the molar ratio to Cl^- .

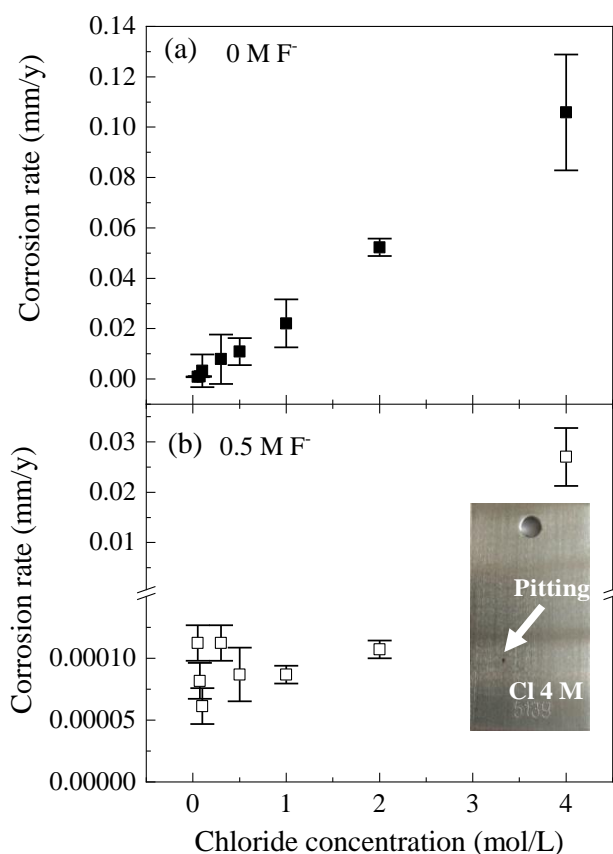


Figure 9. Influence of Cl^- concentration on the corrosion rate of 304 stainless steel (a) in the absence of F^- and (b) with F^- concentration of 0.5 M (30% $(\text{NH}_4)_2\text{SO}_4$, w/v).

The test specimens were washed with deionized water and then cleaned with ethanol. After drying, the surface morphology of the specimens in the different F^- solutions were analyzed by SEM, as shown in Figure 10. In the absence of F^- , there were visible corrosion holes on the surface of the tested specimens, and groove corrosion was observed in some areas (Figure 10(a)). When the F^- concentration was 0.01 M (Figure 10(b)), the corrosion of the stainless steel surface was aggravated, and the corrosion pitting was deeper. On increasing the concentration of F^- , the corrosion pits on the surface of stainless steel gradually reduced, and the corrosion weakened. For 1.0 M F^- (Figure 10(d)), some particle aggregations were observed on the stainless steel surface. The energy spectrum illustrated in Figure 10(d) indicates the presence of the F element on the surface of stainless steel, while the Cl element was negligible. Therefore, when the concentration of F^- is low, there is no

inhibition of corrosion of the stainless steel surface, but when the F^- concentration is high (*i.e.*, ten times that of Cl^- in this work), it can effectively prevent pitting and reduce the uniform corrosion rate by the formation of a F enrichment layer.

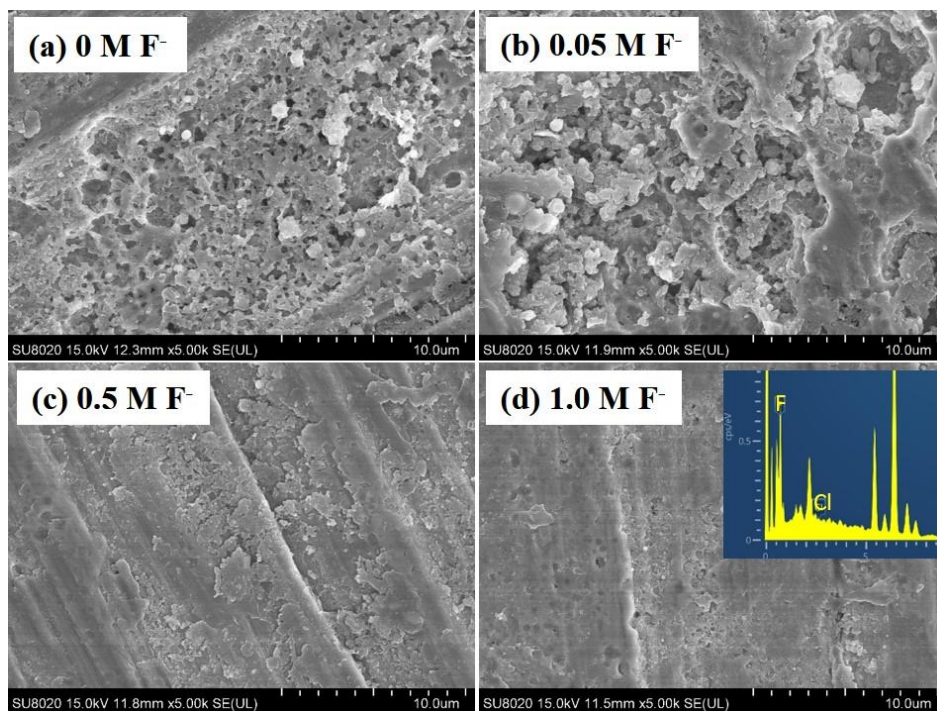


Figure 10. SEM images of 304 stainless steel specimens with the following F^- concentrations: (a) 0 M, (b) 0.05 M, (c) 0.5 M, and (d) 1.0 M (30% $(NH_4)_2SO_4$ (w/v), 0.1 M Cl^-).

XPS was used to analyze the stainless steel surface after immersion, as shown in Figure 11, wherein only the extreme cases have been plotted, *i.e.*, 0 M and 1.0 M F^- . While Cl^- was present in all the experimental solutions, the Cl element was not detected on the surface of the test specimens, indicating that the reaction products containing Cl^- had dissolved in the solution and were washed away in the process of cleaning. After immersion in the 1.0 M F^- solution, the F element was detected on the surface of the stainless steel, as expected. The energy spectrum of the Cr element shows that, compared with the solution without F^- , the binding energy of the stainless steel surface in the solution with 1.0 M F^- had an obvious characteristic peak at about 581 eV, which may be attributed to the complexes formed by Cr and F [29]. According to previous reports, typically, F^- does not lead to pitting corrosion of stainless steel; but on the contrary, it promotes the formation of a passivation film on the stainless steel surface under certain conditions, resulting in a corrosion inhibition effect [12, 19]. The products formed by F^- and dissolved metal ions, which originated from stainless steel, have very low solubility and may even be insoluble in water. For example, if CrF_3 was formed and deposited on the surface of stainless steel, it could inhibit the corrosion anodic reaction [30, 31].

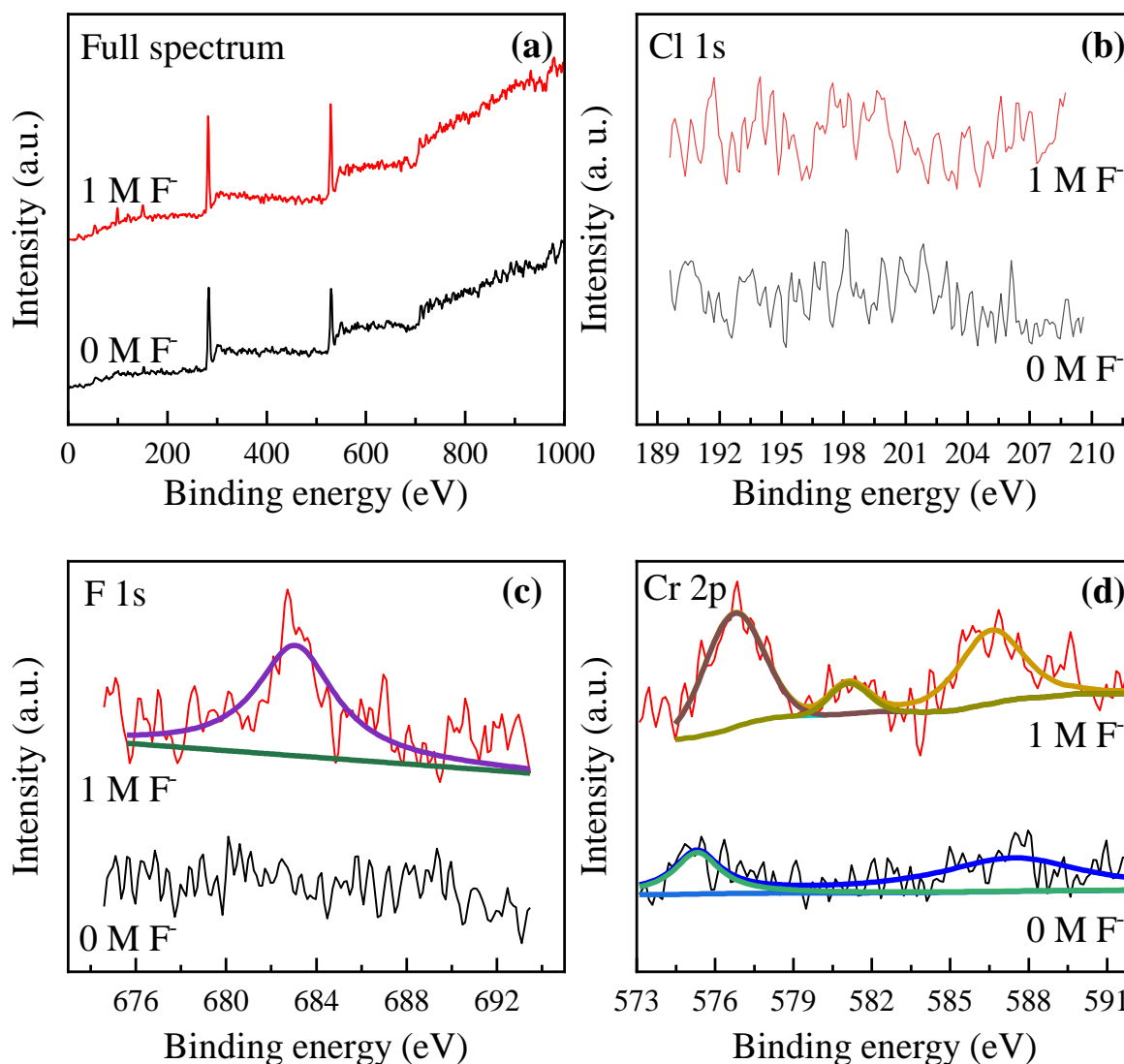


Figure 11. XPS spectra ((a) full spectrum, (b) Cl 1s, (c) F 1s, and (d) Cr 2p) of 304 stainless steel with F^- concentrations of 0 and 1 M, respectively. (30% $(NH_4)_2SO_4$ (w/v), 0.1 M Cl^-)

4. CONCLUSIONS

F^- and Cl^- both cause corrosion of 304 stainless steel when in contact with an ammonia desulphurization slurry; however, at the same time F^- also inhibits the corrosion caused by Cl^- . Under the condition of constant F^- concentration, the increase of Cl^- concentration tends to increase both the general corrosion rate and the probability of pitting corrosion of 304 stainless steel. When the concentration of Cl^- is constant, low concentration of F^- can increase the corrosion rate, while a high concentration of F^- may inhibit the corrosion rate of stainless steel.

When the molar ratio of F^- to Cl^- was 10, the inhibition effect was more significant. The results of the electrochemical test and immersion test showed that when the F^- concentration was relatively high, the uniform corrosion rate of 304 stainless steel could be significantly inhibited, and the

probability of pitting corrosion of stainless steel could be reduced. It is evident that F^- and Cl^- have a significant influence on the pH of the solution. When the concentration of F^- is high, the pH of the solution tends to rise, while Cl^- tends to reduce it. This is related to the dissociation constants of the two ions; F^- tends to combine with hydrogen ions to form HF, which raises the pH. In addition, F^- can react with metal ions to form insoluble sediments, which can inhibit the corrosion of stainless steel.

Therefore, if the concentration of F^- and Cl^- in the ammonia desulfurization slurry can be adjusted using a technical strategy to reduce the Cl^- concentration as far as possible and increase the concentration ratio of F^- and Cl^- , the corrosion rate of desulfurization equipment made of stainless steel may be reduced, and its service time and reliability can be improved.

ACKNOWLEDGMENTS

This work was financially supported by the National Natural Science Foundation of China (Grant Number 21676144).

References

1. Z. Lian, Z. Luo, L. Yuan, M. Guo, W. Wei and K. Liu, *Anti-Corros. Method. M.*, 64 (2017) 432.
2. Y. Yang, L. Guo and H. Liu, *J. Power Sources*, 195 (2010) 5651.
3. L. Niu, R. Guo, C. Tang, H. Guo and J. Chen, *Surf. Coat. Tech.*, 300 (2016) 110.
4. M. Mirjalili, M. Momeni, N. Ebrahimi and M.H. Moayed, *Mat. Sci. Eng. C Mat.*, 33 (2013) 2084.
5. C. Escrivà-Cerdán, E. Blasco-Tamarit, D.M. García-García, J. García-Antón, R. Akid and J. Walton, *Electrochim. Acta*, 111 (2013) 552.
6. V. Alar, A.H. Novak, B. Runje and M. Kurtela, *Mater. Corros.*, 70 (2019) 1273.
7. A.K. Mariano, *Corros. Rev.*, 38 (2020) 1.
8. J.L. Trompette, *Corros. Sci.*, 94 (2015) 288.
9. M.A. Rodríguez, R.M. Carranza and R.B. Rebak, *Metall. Mater. Trans. A*, 36 (2005) 1179.
10. B.R. Tzaneva, L.B. Fachikov and R.G. Raicheff, *Corros. Eng., Sci. Techn.*, 41 (2006) 62.
11. A. Kocijan, D.K. Merl and M. Jenko, *Corros. Sci.*, 53 (2011) 776.
12. I. Martinović, Z. Pilić, I. Dragičević and A. Višekruna, *Int. J. Mater. Res.*, 106 (2015) 1067.
13. B. Löchel, H.H. Strehblow and M. Sakashita, *J. Electrochem. Soc.*, 131 (1984) 522.
14. A. Pardo, M.C. Merino, E. Otero, M.D. López and M.V. Utrilla, *Mater. Corros.*, 51 (2000) 850.
15. N. Meck, S. Day, P. Crook and R. Rebak, *Corrosion*, (2003).
16. Z.B. Wang, H.X. Hu and Y.G. Zheng, *Corros. Sci.*, 130 (2018) 203.
17. R.M. Carranza, M.A. Rodríguez and R.B. Rebak, *Corrosion*, 63 (2007) 480.
18. Y. Yang, L. Guo and H. Liu, *Int. J. Hydrogen Energ.*, 37 (2012) 1875.
19. I.S. Molchan, G.E. Thompson, J. Walton, P. Skeldon, A. Tempez and S. Legendre, *Appl. Surf. Sci.*, 357 (2015) 37.
20. M. Li, C. Zeng, H. Lin and C. Cao, *Brit. Corros. J.* 36 (2001) 179.
21. F. Rosalbino, G. Scavino and G. Ubertalli, *Mater. Corros.*, 71 (2020) 2021.
22. D.G. Li, D.R. Chen and P. Liang, *Int. J. Hydrogen Energ.*, 45 (2020) 30101.
23. S. Zhang, C. Sun and Y. Tan, *Int. J. Electrochem. Sci.*, 15 (2020) 9874.
24. Y. Gui, Z.J. Zheng and Y. Gao, *Thin Solid Films*, 599 (2016) 64.
25. J. Xu, Q. Yang, C. Huang, M.S. Javed, M.K. Aslam and C. Chen, *J. Appl. Electrochem.*, (2017) 1.
26. I. Sekine, H. Usui, S. Kitagawa, M. Yuasa and L. Silao, *Corros. Sci.*, 36 (1994) 1411.
27. P. Klomjit and R.G. Buchheit, *Corros. Rev.*, 38 (2020) 365.
28. I. Ismail, M.K. Harun and M.Z.A. Yahya, *Int. J. Electrochem. Sci.*, 14 (2019) 11491.

29. V.N. Alexander, K. Anna, W.G. Stephen and C.J. Powell, (Eds.), NIST X-ray Photoelectron Spectroscopy Database, NIST Standard Reference Database Number 20, U. S. Department of Commerce, National Institute of Standards and Technology, Gaithersburg, Maryland, (2000).
30. K.M. Forsberg and Å.C. Rasmuson, *J. Cryst. Growth*, 423 (2015) 16.
31. C. Chen, X. Xu, S. Chen, B. Zheng, M. Shui, L. Xu, W. Zheng, J. Shu, L. Cheng and L. Feng, *Mater. Res. Bull.*, 64 (2015) 187.

© 2021 The Authors. Published by ESG (www.electrochemsci.org). This article is an open access article distributed under the terms and conditions of the Creative Commons Attribution license (<http://creativecommons.org/licenses/by/4.0/>).